Volume 5
Number 2
21 January 2023
Pages 303–524

Nanoscale Advances

rsc.li/nanoscale-advances

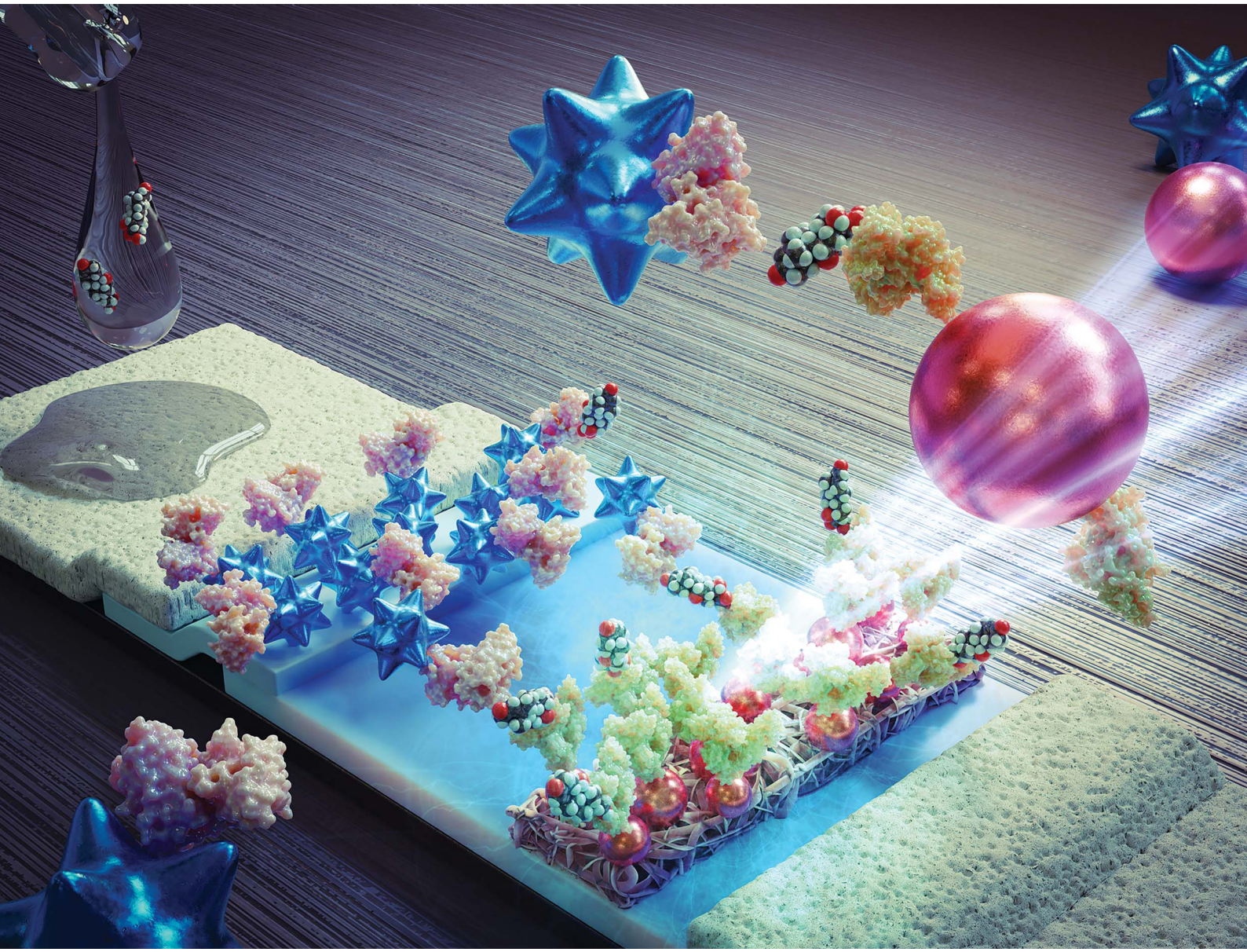

ISSN 2516-0230

ROYAL SOCIETY OF CHEMISTRY

COMMUNICATION
Pier Paolo Pompa *et al.*
A dual-color plasmonic immunosensor for salivary cortisol measurement

NCNST

Nanoscale Advances

ROYAL SOCIETY OF CHEMISTRY

COMMUNICATION

View Article Online
View Journal | View Issue

Cite this: *Nanoscale Adv.*, 2023, **5**, 329

A dual-color plasmonic immunosensor for salivary cortisol measurement†

Anna Scarsi, [ab] Deborah Pedone[a] and Pier Paolo Pompa *[a]

Received 22nd August 2022
Accepted 8th November 2022

DOI: 10.1039/d2na00563h

rsc.li/nanoscale-advances

Lifestyle-related disorders are a public health problem worldwide and their early diagnosis represents the key to successful therapies. In this framework, rapid point-of-care (POC) tests are one of the most promising diagnostic techniques. In particular, the use of saliva is raising increasing interest as a noninvasive biological fluid in POC systems, although the low concentration of salivary biomarkers typically requires strong advances to improve the device sensitivity. In this study, the plasmonic properties of two differently shaped gold nanoparticles (*i.e.*, nanospheres and nanostars) were combined to develop an efficient paper-based immunosensor for the naked-eye evaluation of salivary cortisol, known as one of the main stress-related biomarkers. Notably, the dual-color system facilitated an immediate and easy evaluation of cortisol levels, based on a blue-to-pink color change of the detection zone. Furthermore, the implemented strategy showed potential applicability as a rapid and portable monitoring system, allowing discriminating different target concentrations.

1 Introduction

The growing incidence of lifestyle-related disorders is one of the main concerns of modern society.[1] To date, prevention and early detection represent a crucial strategy for effective therapies.[2] In this framework, point-of-care (POC) testing is finding increasing applications as a rapid and portable diagnostic technique, allowing the detection of a variety of relevant biomarkers in biological fluids.[3–5] Among them, blood represents one of the most employed, due to the presence of numerous targets and their large availability in terms of concentration.[6] However, the use of such biological fluid has also some drawbacks, primarily because it is invasive and may require specialized personnel and instrumental steps. For these reasons, interest in using noninvasive biological fluids is strongly increasing.[7] In particular, saliva is suitable for POC testing since it is easy to use in sampling and to handle, but it is also a challenging fluid given the 100–1000 times lower concentrations of biomarkers with respect to blood, thus requiring the development of very sensitive detection strategies.[7,8]

In this context, cortisol is a stress-related biomarker with a strong serum–saliva correlation, even though salivary concentrations are in the nanomolar range.[9] Cortisol is a steroid hormone produced by adrenal glands as the end product of the hypothalamic–pituitary–adrenal axis, the central stress-response system of the body.[10] It plays a key role in the regulation of many physiological processes and in the maintenance of homeostasis.[7,10] Cortisol level alterations induced by psychological issues can lead to serious pathological conditions,[7,10] making POC technologies necessary to ensure frequent screening and early medical diagnosis.

POC salivary cortisol measurement has been recently reported by means of different detection methodologies, including electrochemical determination,[2,11] aptasensing,[2,12] and immunoassay strategies.[13] Among the latter ones, the lateral flow assay (LFA) is the most employed technique. The core of this technology relies on the capillary flow of the sample through a nitrocellulose strip up to the test line, after the interaction with a probe. Depending on the detection probe, cortisol can be measured in LFA exploiting aptamers[14] or most commonly antibodies in the so-called lateral flow immunoassay (LFIA), where the readout is colorimetric,[15] or based on chemiluminescence[16] or on the use of smartphone applications.[17]

In this work, we developed a dual-color plasmonic LFIA as a rapid and easy-to-use (instrument-free) salivary cortisol monitoring system, combining two differently shaped plasmonic gold nanoparticles (*i.e.*, nanospheres and nanostars). This innovative strategy facilitates the naked-eye evaluation of cortisol levels in the POC system, thanks to a clear readout

[a]*Nanobiointeractions & Nanodiagnostics, Istituto Italiano di Tecnologia (IIT), Via Morego, 30, Genova 16163, Italy. E-mail: pierpaolo.pompa@iit.it*

[b]*Department of Chemistry and Industrial Chemistry, University of Genoa, Via Dodecaneso, 31, Genova 16146, Italy*

† Electronic supplementary information (ESI) available. See DOI: https://doi.org/10.1039/d2na00563h

based on a blue-to-pink color change of the test line, in contrast to the typical color intensity increase/decrease, which requires a more difficult interpretation and/or comparison with reference standards.

2 Results and discussion

2.1 Design and working principle of the dual-color plasmonic LFIA

Given the small size of the cortisol molecule (MW ≈ 360 g mol^{-1}), a competitive LFIA was developed.[18] The assay is schematized in Fig. 1a. The device was composed of a series of pads applied onto a nitrocellulose membrane[18] (see Materials and methods for details). In particular, the saliva drops were added on the sample pad. Then, the sample started to flow through the strip and reached the conjugate pad, where we deposited the detection bioreceptor, namely the AuNS–Ab conjugate, constituted by a monoclonal anti-cortisol antibody (Ab) adsorbed on 60 nm gold nanostars (AuNSs).[19,20] During the test run, the Ab interacted with the salivary cortisol present in the sample. Finally, the flow reached the detection zone (test line), consisting of a 35 nm gold nanosphere (AuNP)–bovine serum albumin (BSA)–cortisol conjugate. The absorbent pad, placed at the end of the strip, ensured the driving force for the flow. Owing to the plasmonic properties of the gold nanoparticles and their molar extinction coefficients (ε),[21,22] the 60 nm AuNSs showed a blue color (UV-vis peak around 650 nm, Fig. 1b blue curve, right vial), while the 35 nm AuNPs[23,24] appeared red (UV-vis peak around 525 nm, Fig. 1b red curve, left vial) (additional characterizations of the AuNPs and AuNSs are reported in Fig. S1 and S2†). In the presence of physiological

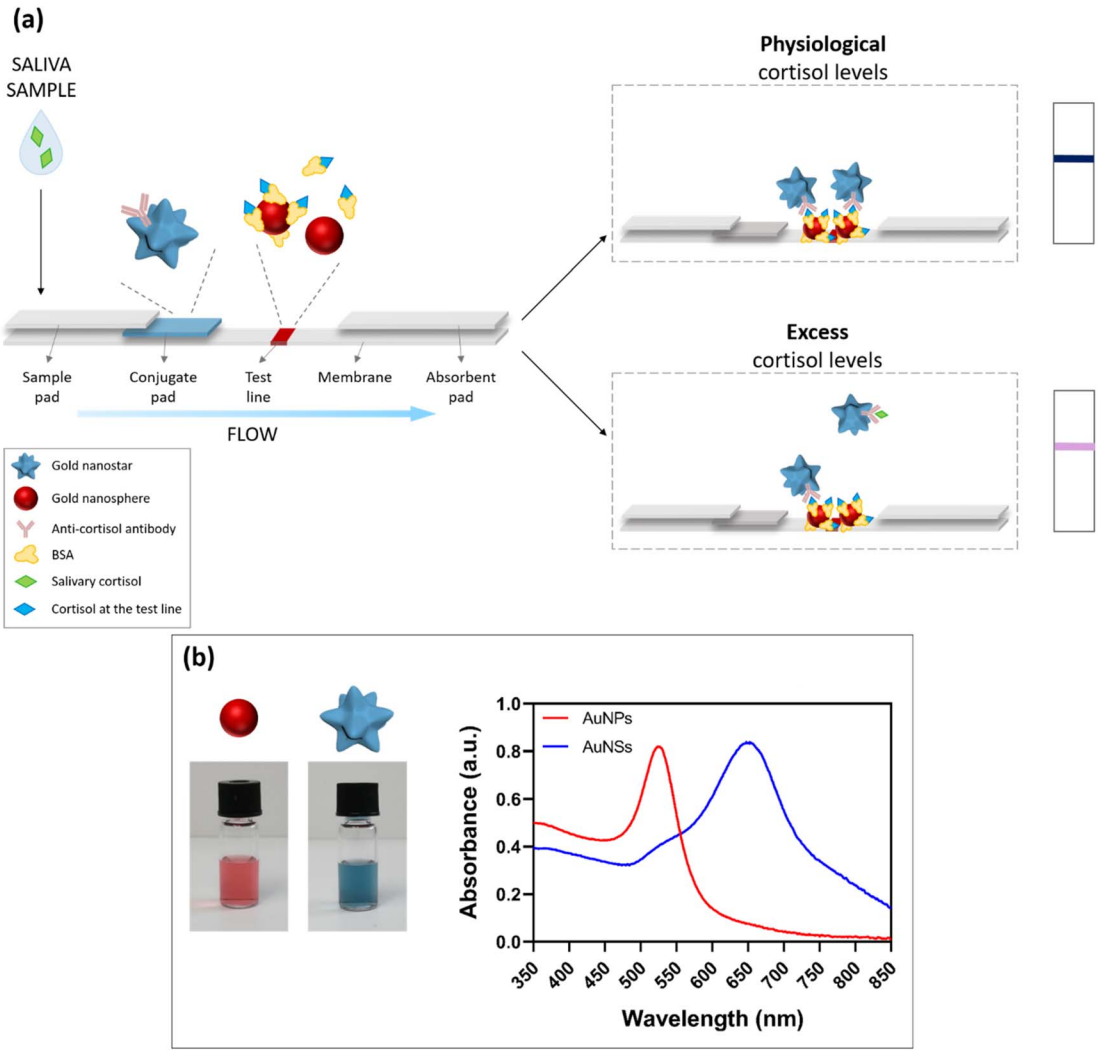

Fig. 1 Design and working principle of the dual-color plasmonic LFIA device. (a) Scheme of the proposed POC system, based on the combination of gold nanospheres (AuNPs) and nanostars (AuNSs). In the presence of physiological cortisol levels in saliva, the AuNS–Ab conjugates will bind to the AuNP–BSA–cortisol complexes immobilized in the detection zone, resulting in the formation of a blue test line. When the cortisol levels are in excess, the AuNS–Ab conjugates will interact with salivary cortisol during the run along the strip, leading to a minor quantity of AuNS–Ab bound at the detection zone, with a resulting pink/light purple color of the test line. (b) The bottom panel displays the plasmonic properties of the two types of gold nanoparticles employed: AuNPs showed an absorption peak around 525 nm, resulting in a red color of the corresponding aqueous suspension (left vial); AuNSs showed a plasmon peak around 650 nm, leading to a blue-colored suspension (right vial).

cortisol levels (Fig. 1a, top scheme), a higher quantity of detection bioreceptor was available to bind cortisol at the test line, leading to the accumulation of AuNSs at the detection zone with a consequent formation of a blue test line, given the higher ε of the AuNSs with respect to the AuNPs' one. Conversely, when the salivary cortisol levels were in excess (Fig. 1a, bottom scheme), a larger fraction of AuNS–Ab interacted with cortisol during the run, leaving a minor quantity of detection bioreceptor available for the binding at the test line. Therefore, the resulting color of the line was pink/light purple due to the higher contribution of the red baseline in these conditions. Exploiting the color change of the test line, this dual-color system allows for easier naked-eye detection of the biomarker's concentration in the sample, as compared to traditional competitive LFIA, in which the amount of the target is inversely proportional to the intensity of the test line, and each condition is evaluated by observing the color intensity decrease with the concentration of target increasing.

Some dual-color systems have been recently reported in the literature exploiting both naked-eye[25–28] and fluorescence-based[29] detection. In the colorimetric methods, different colors are used to better distinguish between the test and control lines (and for the target evaluation based on the T/C ratio after the instrumental readout), or they allow the evaluation of different targets using multiple test lines. On the other hand, fluorescence-based approaches require various instrumental setups, with excitation sources and optical detectors. Notably, none of the above systems provide for the direct naked-eye detection of the analytes of interest through a target-induced color change at the detection zone. In our system, by combining two different plasmonic nanomaterials at the test line, we tried to facilitate the visual detection of the biomarker through the color change that takes place when increasing the concentration of the target in the sample. In particular, the above-threshold level of salivary cortisol was highlighted by the appearance of a red color in the blue test line, which became more intense when increasing the cortisol concentration, giving a pink shade to the test line. Hence, this approach allows an immediate and clearer semi-quantitative evaluation of salivary cortisol compared to traditional single-color LFIA, based on the intensity decrease of the test line with respect to reference standards.

2.2 AuNS–Ab conjugate optimization and characterization

In order to determine the optimal functionalization conditions in terms of the antibody concentration, pH of the solution, and conjugation time, the gold aggregation test (GAT) was performed.[18] GAT exploits the tendency of gold nanoparticles to aggregate in the presence of high salt concentrations, and can be used to evaluate the Ab-induced particle stabilization effect. The aggregation rate can be monitored by UV-vis spectroscopy.

All conjugation procedures were performed using gold nanostars at 0.7 O.D.,[18] and by varying the pH value of the solution (7, 8, 9), antibody concentration (0, 30, 50, 100, 200 μg mL^{-1}), and nanostar-antibody incubation time (20 and 60 min). The experimental results showed that all the above parameters strongly affected the nanostar conjugation effect. When AuNSs were not sufficiently stabilized by the antibody conjugation, they quickly aggregated in the presence of NaCl. With progressively increasing the antibody concentration, a higher stability of AuNSs was observed. Notably, 50 μg mL^{-1} was the optimal Ab concentration to ensure high particle stability in the experimental conditions used. Similarly, a pH value of 8–9 was necessary for a complete saturation of the gold nanostar surface and for effective nanoparticle stabilization. Finally, the most stable conjugates were obtained using long incubation times (1 h), likely due to the higher presence of antibodies on the nanostar surface.

After the conjugation, the AuNS–Ab complex was purified by centrifugation and the resulting pellet was resuspended in the conjugate pad buffer (see Materials and methods for details). The conjugation was characterized by DLS (Fig. S1c†) and UV-vis (Fig. S1d†), confirming the conjugate monodispersity and stability.

2.3 AuNP–BSA–cortisol conjugate characterization

The conjugation was performed in two steps (see Materials and methods for details). First, we prepared a BSA-cortisol complex in PBS alkaline solution. After 2 h of incubation at room temperature, we added the gold nanospheres suspension and we left the mixture stirring for 2 h. The final AuNP–BSA–cortisol conjugate was characterized by DLS (Fig. S2c†) and UV-vis (Fig. S2d†), showing stability and low polydispersity. The conjugate was then striped onto a nitrocellulose membrane at the detection zone.

2.4 LFIA strip optimization

To ensure a homogeneous flow along the device and a rapid and effective target–probe interaction, the accurate selection and optimization of materials and procedures were performed. In particular, considering the size of the AuNS–Ab conjugate (Fig. S1c†), a medium flow rate nitrocellulose membrane was preferred to faster membranes. Furthermore, the effect of the pads pretreatment with proper buffers was investigated. It was found that the resuspension of the detection probe in a buffer solution containing stabilizing and solubilizing agents, such as BSA and sucrose,[18] helped to preserve the Ab conformation and guaranteed an immediate resuspension of the NSs. Also, the use of detergents- and saturating agents-based buffers as pre-treatments for the sample and detection pads[18] facilitated the flow of the sample along the membrane, as well as the antigen–antibody recognition.

All these optimizations were performed on real saliva samples. Since the detection was designed to be semi-quantitative, we observed that it was not possible to use whole untreated saliva, due to the high sample-to-sample viscosity variations,[4] which led to heterogeneous flows and recognition issues at the detection zone. Therefore, in the attempt to minimize the viscosity variations in each sample, we optimized a simple and rapid (*ca.* 30 s) pre-filtration step using cellulose acetate syringe filters (0.2 μm pore size). Such a procedure allowed us to remove the mucins and obtain samples suitable for more controlled runs through the nitrocellulose strip. The

filtration was easily performed in a single-step operation and required about 1 mL of whole saliva. This fast method is preferable to other types of sample pretreatment, which usually involve centrifugation steps.[30–32]

2.5 Evaluation of cortisol in saliva samples

The optimized LFIA was then applied in a proof-of-concept experiment to determine the cortisol level in saliva samples (Fig. 2). All the pictures reported in the following were acquired using a standard smartphone camera in non-controlled light conditions, to simulate a real application. Before the test, the device showed a red baseline corresponding to the AuNP–BSA–cortisol complex deposited onto the test line (Fig. 2a). As anticipated in the description of Fig. 1a, the final LFIA conditions were experimentally optimized taking into account the molar extinction coefficients (ε) of the two nanomaterials employed. Since AuNSs have a higher ε than AuNPs, in the presence of a large quantity of AuNSs captured on the detection zone (namely in the physiological range of salivary cortisol), the test line appeared blue. In contrast, in the presence of higher cortisol levels in the salivary samples, the excess cortisol binds the AuNS–Ab conjugate during the run, competing with the AuNP–BSA–cortisol complex immobilized in the test line, which then starts to become pink/purple, due to the lower amount of gold nanostars bound on such region.

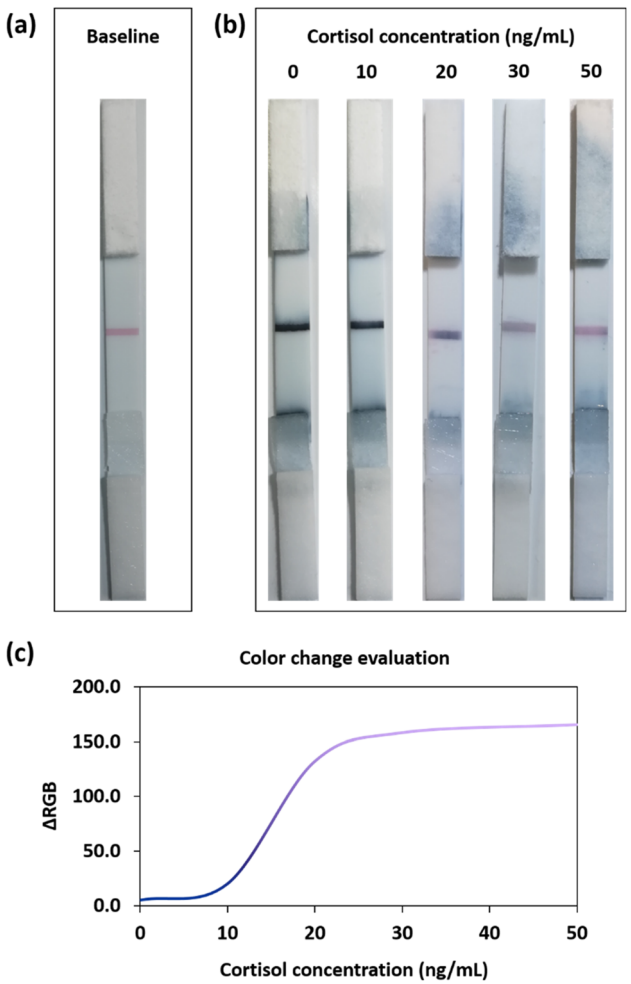

Fig. 2 Cortisol levels evaluation in saliva samples. (a) Representative picture of the dual-color LFIA device before the test, showing the red baseline in the test line, corresponding to the AuNP–BSA–cortisol conjugate. (b) Representative pictures of the POC devices probe results with cortisol concentrations ranging from 0 to 50 ng mL^{-1}. At physiological concentrations of cortisol (up to 10 ng mL^{-1}), the test line appeared blue. When increasing the level of the hormone spiked in saliva samples (around 20 ng mL^{-1}), the competition for the detection bioreceptor started to occur and the red baseline became visible, eliciting an overall violet color of the test line. In the presence of higher levels of cortisol (30–50 ng mL^{-1}), the color of the gold nanospheres clearly prevailed, with a resulting pink/reddish test line. (c) The color change could be also easily evaluated using a standard smartphone camera, by ΔRGB analysis, showing an evident color transition above the physiological range of salivary concentration.

Cortisol is released in the organism following a circadian rhythm with a maximum concentration peak in the morning, approaching *ca.* 10 ng mL^{-1} in saliva.[9,10,17,33] We thus considered such concentration as a cut-off value between physiological and non-physiological (excess) levels; consequently, with our LFIA device, we tested the 0–50 ng mL^{-1} range.[9,34] The samples were prepared by spiking different concentrations from a cortisol standard solution into saliva samples from several healthy donors.

At physiological levels of cortisol (up to 10 ng mL^{-1}), most of the detection bioreceptors were available for the interaction with the AuNP–BSA–cortisol complex at the detection zone, providing a dark-blue test line (Fig. 2b). On the other hand, when increasing the concentration of the biomarker (20 ng mL^{-1}), the excess cortisol present in the saliva sample competed, during the run, for the binding to the AuNS–Ab conjugate with the cortisol at the test line. In this latter case, since a minor quantity of detection bioreceptor binds to the test line, the red baseline started to become visible. When the cortisol levels were in large excess (pathological conditions, 30–50 ng mL^{-1}) the majority of the detection bioreceptors binds to the salivary cortisol, resulting in a pink test line given by the higher contribution of the red baseline. Hence, owing to the dual-color strategy of our plasmonic immunosensor, it was possible to easily assess salivary cortisol levels by observing the blue-to-pink color change at the detection zone.

This evaluation could also be performed by using a standard smartphone camera and subsequent RGB analysis of the photos of the POC devices. In particular, Fig. 2c shows the ΔRGB plot in the analyzed range of the cortisol levels (0–50 ng mL^{-1}). The colorimetric method allowed discriminating among the three main regions inside the dynamic range. At low cortisol levels (0–10 ng mL^{-1}), the blue signal had high intensity, and the samples in this concentration interval could be assimilated to a negative control. Medium cortisol levels (15–25 ng mL^{-1}) resulted in more purple test lines, suggesting the presence of stress conditions or inflammatory states in the tested organism. At high cortisol levels (30–50 ng mL^{-1}), the test line appeared clearly pink/reddish, and this could indicate severe pathological conditions.

The reliability of the colorimetric device was then tested on different saliva samples (n = 9) to assess the analytical

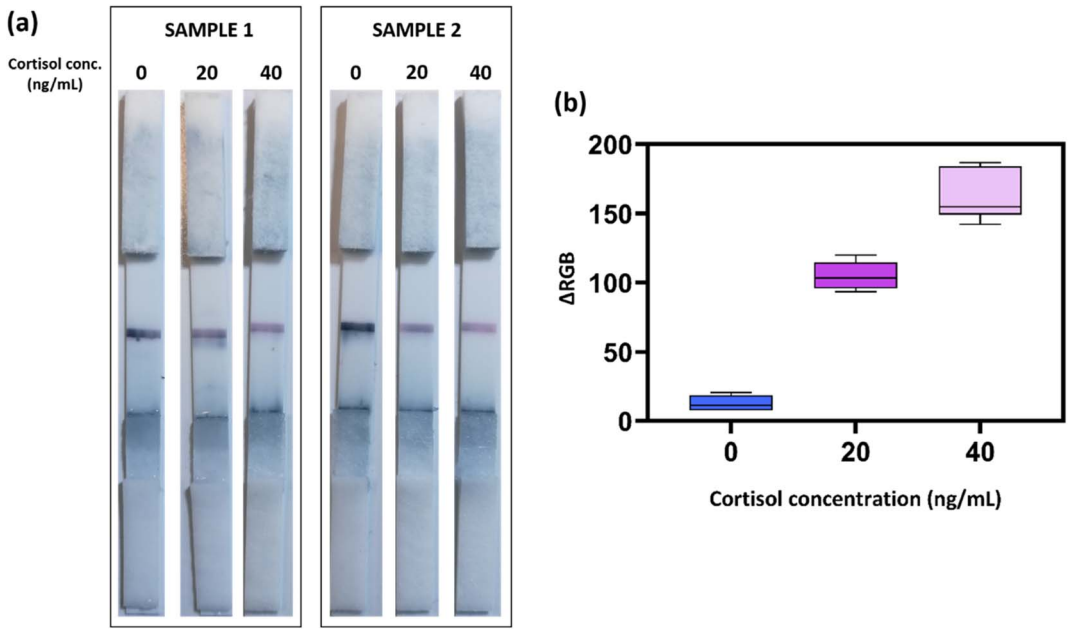

Fig. 3 Representative experiments on different saliva samples ($n = 9$). (a) Representative pictures of samples 1 and 2 tested at three different cortisol concentrations (0, 20, and 40 ng mL^{-1}). (b) ΔRGB analysis performed on nine saliva samples in the 0–40 ng mL^{-1} concentration range. The average value and the min-to-max bar are reported for each tested concentration.

performance of the POC system when probed with real and heterogeneous samples from different donors. Fig. 3a reports the results of two representative samples. Interestingly, a clear color change was obtained in both biological samples in the relevant concentration range. Moreover, a broader evaluation of the nine test individuals confirmed the correct colorimetric response of the LFIA device (Fig. 3b), indicating that the combination of the simple pre-filtration step of the saliva (to prevent viscosity variations), the accurate selection and optimization of the employed antibodies, and the dual-color approach could guarantee a reliable POC system for fast, noninvasive, and instrument-free cortisol assessment. The observation of these results also revealed the absence of significant unspecific binding issues, since the test provided very similar colorimetric results at each cortisol concentration in the different samples.

As a control experiment against a typical single-color LFIA, we developed a similar POC device by exploiting only the AuNSs as the detection bioreceptors, namely without the red baseline composed by the nanosphere conjugates. In this case, as clearly shown in Fig. S3,† the presence of high non-physiological levels of salivary cortisol was more difficult to assess, since such levels caused an intensity decrease of the blue color at the test line. However, such different decreases were quite challenging to evaluate in the absence of clear reference intensity standards or automated readout equipment, unlike the more direct visual evidence provided by the dual-color system.

Finally, we designed a prototype version of the dual-color immunoassay, which included also a control line, to prevent possible misinterpretations of the colorimetric results. In particular, in the control line, we immobilized protein G, which has high affinity for IgG (the anti-cortisol antibody used in this study is an IgG isotype).[35] We tested such integrated devices with a real saliva sample at 0 and 50 ng mL^{-1} of cortisol (as reported in Fig. S4†). In this configuration, it was possible to clearly distinguish between excess cortisol conditions and no sample/not properly working devices, allowing a better interpretation of the colorimetric readout (*e.g.*, avoiding possible false-positive results).

3 Conclusions

In this work, we developed an innovative dual-color competitive lateral flow immunoassay for salivary cortisol evaluation, based on the use of two differently shaped gold nanoparticles, namely nanospheres and nanostars. The plasmonic properties of the two particles were exploited to get a target-modulated blue-to-pink color change that allowed an easy and fast naked-eye assessment of the cortisol levels in saliva. By this approach, we were able to identify three main color regions corresponding to three relevant ranges of salivary cortisol, namely physiological conditions, mid inflammatory/stress response, and pathological conditions, using a cut-off value of 10 ng mL^{-1} salivary concentration. The POC device was tested on real samples from different donors, using a simple and rapid pre-filtration step, and the color change was evaluated through visual detection and RGB analysis. This further confirmed the advantages of the dual-color plasmonic system with respect to traditional color-fading competitive lateral flow immunoassays. The proposed mechanism showed potential applicability as rapid and easy-to-use POC technology for the naked-eye, noninvasive evaluation of cortisol levels.

4 Materials and methods

4.1 Chemicals and materials

All the chemicals and reagents employed were of high technical grade, stored following the vendor recommendations, and directly used with no further purification.

Hydroxylamine sulfate ($(NH_2OH)_2 \cdot H_2SO_4$) and hydrogen tetrachloroaurate ($HAuCl_4 \cdot xH_2O$, Au 49% min) were purchased from Alfa Aesar. Sodium citrate tribasic dihydrate ($C_6H_5Na_3O_7 \cdot 2H_2O$, BioUltra, for molecular biology, ≥99.5%), phosphate buffered saline (tablet), HEPES ($C_8H_{18}N_2O_4S$, BioPerformance Certified, ≥99.5% (titration), suitable for cell culture), hydrocortisone ($C_{21}H_{30}O_5$, BioReagent, suitable for cell culture), bovine serum albumin (heat shock fraction, protease free, fatty acid free, essentially globulin free, pH 7, ≥98%), sucrose ($C_{12}H_{22}O_{11}$, BioUltra, for molecular biology, ≥99.5% (HPLC)), Tween 20 ($C_{58}H_{114}O_{26}$,viscous liquid), sodium dodecyl sulfate ($C_{12}H_{25}O_4S.Na$, BioUltra, for molecular biology, ≥99.0% (GC)), and ethanol (C_2H_6O, puriss., meets analytical specification of Ph. Eur., BP, 96.0–97.2%) were purchased from Merck (Sigma-Aldrich). Anti-cortisol antibody [XM210] (Mouse monoclonal [XM210] to Cortisol) and recombinant protein G were purchased from Abcam.

The sample pad (grade 319, composition Cotton Fibers), conjugate pad (grade 8980, composition Chopped Glass w/ Binder), and absorbent pad (grade 440, composition Cotton/Glass Blend) were purchased from Ahlstrom-Munksjö. Nitrocellulose membrane (Whatman FF120HP, 25 mm × 50 m) was purchased from GE Healthcare Life Sciences (Cytiva).

All the solutions and buffers were prepared using ultrapure deionized water (MilliQ).

4.2 Synthesis and characterization of the gold nanoparticles

Spherical 15 nm citrate-capped gold nanoparticles (AuNPs) were synthesized by the Turkevich–Frens method[36,37] as seeds for preparation of the 35 nm AuNPs and 60 nm gold nanostars (AuNSs). Briefly, 25 mL of trisodium citrate solution 40 mM was added to a boiling solution of hydrogen tetrachloroaurate 1 mM under vigorous stirring. After 12 min, the colloidal suspension was cooled down to room temperature, filtered, and stored at 4 °C for further use.

Next, 35 nm AuNPs and 60 nm AuNSs were synthesized by the wet chemical reduction of 15 nm seeds in water, following established protocols with some optimizations (the seed volume was adjusted to get the desired size of 35 nm AuNPs, and HEPES volume was reduced to give AuNSs with shorter tips, more suitable for conjugation with the antibody).[38,39]

The morphological and dimensional characterizations of AuNPs and AuNSs were performed by DLS (Malvern-PANalytical), UV-vis spectrophotometry (Thermo Fisher NanoDrop®, wavelength accuracy ± 1 nm, absorbance accuracy 3% at 0.74 Abs @ 350 nm), and TEM (JEOL JEM-1400Plus TEM, with LaB_6 thermionic source and maximum acceleration voltage 120 kV). The nanoparticles' size was determined by measuring at least 150 nanoparticles using ImageJ software (NIH).

4.3 Preparation of the gold nanoparticle-based conjugates

4.3.1 AuNS–Ab conjugate. First, 1 mL of antibody solution 9.36 μg mL^{-1} in borate buffer 5 mM at pH 8.6 was prepared. Then, AuNSs were added up to 2.1 O.D. The mixture was incubated at room temperature for 1 h under stirring (600 rpm) and then centrifuged (3900 rcf, 10 min, 4 °C). The pellet was resuspended in conjugate pad buffer.

4.3.2 AuNP–BSA–cortisol conjugate. First, a BSA-cortisol conjugate was prepared. Cortisol 0.4 mg mL^{-1} in ethanol was added to a solution of BSA 4 mg mL^{-1} in PBS 10 mM at pH 7.6. The mixture was incubated at room temperature for 2 h at 600 rpm. After that, a solution of AuNPs 0.87 nM was added and incubated for another 2 h under the same conditions. The final mixture was striped as the test line onto a nitrocellulose membrane, by using a Biodot XYZ S-series V3.11 (dispense rate of 0.625 μL cm^{-1} and a speed of 50 mm s^{-1}).

4.4 Control line deposition

Here, 0.5 μL of a solution of protein G (0.2 mg mL^{-1}) in PBS was deposited onto each membrane at a distance of *ca.* 4 mm from the test line, to perform the experiments illustrated in Fig. S4.†

4.5 Lateral flow pads pretreatment[18]

4.5.1 Sample pad. 10 min soaking in sample pad buffer (PBS 10 mM pH 7.4, 0.05% SDS, 0.05% BSA) → 1 h drying at 37 °C → 1 h drying under vacuum.

4.5.2 Conjugate pad. Deposition of detection bioreceptor solution in conjugate pad buffer (PBS 10 mM pH 7.4, 5% sucrose, 1% BSA, 0.5% Tween 20) → 2 h drying under vacuum.

4.5.3 Nitrocellulose membrane. 1 × 20 min blocking (PBS 10 mM pH 7.4 1% BSA) → 2 × 10 min washing (PBS 5 mM 0.05% Tween 20) → 1 h drying at 37 °C → 2 h drying under vacuum.

4.6 Assay procedure and data collection

Unstimulated saliva samples were collected from nine healthy volunteers at least 1 h after eating, drinking, and performing oral hygiene procedures.[22] The samples were filtered using a 0.2 μm acetate cellulose syringe filter to remove mucins, and then spiked with 20 μL of cortisol standard solutions, to get a dynamic range from 0 to 50 ng mL^{-1}. Next, 75 μL of each sample was added drop by drop onto the sample pad. Each result was evaluated at 15 min and a picture of every test line was acquired, using a Huawei P10-lite smartphone camera in non-controlled light conditions, to better reproduce a real-case employment of the device.

RGB coordinates were acquired at each test line using ImageJ software (NIH) and the ΔRGB values were obtained employing this previously published eqn:[19]

$$\Delta RGB = \sqrt{(R_{t1} - R_{t0})^2 + (G_{t1} - G_{t0})^2 + (B_{t1} - B_{t0})^2}$$

Ethical statement

All subjects gave written informed consent for the inclusion in this study. The protocol of the research study was approved by the Ethical Committee of Regione Liguria (405/2020-DB id 10787).

Conflicts of interest

The authors declare no conflicts of interest.

Acknowledgements

This work has been partially supported by Italian Space Agency (ASI) through the MARS-PRE Project. The authors gratefully acknowledge Paolo Donati, Tania Pomili, Helena Torné-Morató, and Giuseppina Tatulli for useful discussions and help during experiments.

References

1 Fatma Al-Maskari, *Lifestyle Diseases: An Economic Burden on the Health Services*, 2010, **https://www.un.org/en/chronicle/article/lifestyle-diseases-economic-burden-health-services**.
2 A. S. Zainol Abidin, *et al.*, Current and Potential Developments of Cortisol Aptasensing towards Point-of-Care Diagnostics (POTC), *Sensors*, 2017, **17**(5), 1180, DOI: **10.3390/s17051180**.
3 A. Sharma, A. I. Y. Tok, P. Alagappan and B. Liedberg, Point of care testing of sports biomarkers: Potential applications, recent advances and future outlook, *TrAC, Trends Anal. Chem.*, 2021, **142**, 116327, DOI: **10.1016/j.trac.2021.116327**.
4 O. Miočević, *et al.*, Quantitative Lateral Flow Assays for Salivary Biomarker Assessment: A Review, *Front. Public Health*, 2017, **5**, 133, DOI: **10.3389/fpubh.2017.00133**.
5 L. Boselli, T. Pomili, P. Donati and P. P. Pompa, Nanosensors for Visual Detection of Glucose in Biofluids: Are We Ready for Instrument-Free Home-Testing?, *Materials*, 2021, **14**, 1978.
6 W. Londeree, K. Davis, D. Helman and J. Abadie, Bodily fluid analysis of non-serum samples using point-of-care testing with iSTAT and Piccolo analyzers *versus* a fixed hospital chemistry analytical platform, *Hawaii J. Med. Public Health*, 2014, **73**, 3–8.
7 G. Giacomello, A. Scholten and M. K. Parr, Current methods for stress marker detection in saliva, *J. Pharm. Biomed. Anal.*, 2020, **191**, 113604, DOI: **10.1016/j.jpba.2020.113604**.
8 D. Pedone, M. Moglianetti, M. Lettieri, G. Marrazza and P. P. Pompa, Platinum Nanozyme-Enabled Colorimetric Determination of Total Antioxidant Level in Saliva, *Anal. Chem.*, 2020, **92**, 8660–8664, DOI: **10.1021/acs.analchem.0c01824**.
9 M. Zangheri, *et al.*, Chemiluminescence-based biosensor for monitoring astronauts' health status during space missions: Results from the International Space Station, *Biosens. Bioelectron.: X*, 2019, **129**, 260–268, DOI: **10.1016/j.bios.2018.09.059**.
10 A. Kaushik, A. Vasudev, S. K. Arya, S. K. Pasha and S. Bhansali, Recent advances in cortisol sensing technologies for point-of-care application, *Biosens. Bioelectron.: X*, 2014, **53**, 499–512, DOI: **10.1016/j.bios.2013.09.060**.
11 A. Gevaerd, E. Y. Watanabe, C. Belli, L. H. Marcolino-Junior and M. F. Bergamini, A complete lab-made point of care device for non-immunological electrochemical determination of cortisol levels in salivary samples, *Sens. Actuators, B*, 2021, **332**, 129532, DOI: **10.1016/j.snb.2021.129532**.
12 F. Mortazavi Moghadam, M. Bigdeli, A. Tamayol and S. R. Shin, TISS nanobiosensor for salivary cortisol measurement by aptamer Ag nanocluster SAIE supraparticle structure, *Sens. Actuators, B*, 2021, **344**, 130160, DOI: **10.1016/j.snb.2021.130160**.
13 A. Apilux, S. Rengpipat, W. Suwanjang and O. Chailapakul, Paper-based immunosensor with competitive assay for cortisol detection, *J. Pharm. Biomed. Anal.*, 2020, **178**, 112925, DOI: **10.1016/j.jpba.2019.112925**.
14 S. Dalirirad, D. Han and A. J. Steckl, Aptamer-Based Lateral Flow Biosensor for Rapid Detection of Salivary Cortisol, *ACS Omega*, 2020, **5**, 32890–32898, DOI: **10.1021/acsomega.0c03223**.
15 H.-K. Oh, K. Kim, J. Park, H. Jang and M.-G. Kim, Advanced trap lateral flow immunoassay sensor for the detection of cortisol in human bodily fluids, *Sci. Rep.*, 2021, **11**, 22580, DOI: **10.1038/s41598-021-02084-7**.
16 S. Choi, *et al.*, Real-time measurement of human salivary cortisol for the assessment of psychological stress using a smartphone, *Sens. Bio-Sens. Res.*, 2014, **2**, 8–11, DOI: **10.1016/j.sbsr.2014.08.001**.
17 M. Zangheri, *et al.*, A simple and compact smartphone accessory for quantitative chemiluminescence-based lateral flow immunoassay for salivary cortisol detection, *Biosens. Bioelectron.: X*, 2015, **64**, 63–68, DOI: **10.1016/j.bios.2014.08.048**.
18 C. Parolo, *et al.*, Tutorial: design and fabrication of nanoparticle-based lateral-flow immunoassays, *Nat. Protoc.*, 2020, **15**, 3788–3816, DOI: **10.1038/s41596-020-0357-x**.
19 P. Donati, T. Pomili, L. Boselli and P. P. Pompa, Colorimetric Nanoplasmonics to Spot Hyperglycemia From Saliva, *Front Bioeng Biotechnol.*, 2020, **8**, 601216, DOI: **10.3389/fbioe.2020.601216**.
20 H. Torné-Morató, P. Donati and P. P. Pompa, Nanoplasmonic Strip Test for Salivary Glucose Monitoring, *Nanomaterials*, 2022, **12**, 105.
21 Z. Zhang, *et al.*, Plasmonic colorimetric sensors based on etching and growth of noble metal nanoparticles: Strategies and applications, *Biosens. Bioelectron.: X*, 2018, **114**, 52–65, DOI: **10.1016/j.bios.2018.05.015**.
22 T. Pomili, P. Donati and P. P. Pompa, Paper-Based Multiplexed Colorimetric Device for the Simultaneous Detection of Salivary Biomarkers, *Biosensors*, 2021, **11**, 443.
23 P. Valentini, *et al.*, DNA Barcoding Meets Nanotechnology: Development of a Universal Colorimetric Test for Food

Authentication, *Angew. Chem., Int. Ed.*, 2017, **56**, 8094–8098, DOI: **10.1002/anie.201702120**.

24 S. Franco-Ulloa, *et al.*, Dispersion state phase diagram of citrate-coated metallic nanoparticles in saline solutions, *Nat. Commun.*, 2020, **11**, 5422, DOI: **10.1038/s41467-020-19164-3**.

25 S. Cavalera, F. Di Nardo, L. Forte, F. Marinoni, M. Chiarello, C. Baggiani and L. Anfossi, Switching from multiplex to multimodal colorimetric lateral flow immunosensor, *Sensors*, 2020, **20**, 6609.

26 M. Zhu, *et al.*, A highly sensitive dual-color lateral flow immunoassay for brucellosis using one-step synthesized latex microspheres, *Anal. Methods*, 2019, **11**, 2937–2942, DOI: **10.1039/C9AY00944B**.

27 M. Zhu, *et al.*, Ultrasensitive dual-color rapid lateral flow immunoassay *via* gold nanoparticles with two different morphologies for the serodiagnosis of human brucellosis, *Anal. Bioanal. Chem.*, 2019, **411**, 8033–8042, DOI: **10.1007/s00216-019-02156-8**.

28 F. Di Nardo, *et al.*, Colour-encoded lateral flow immunoassay for the simultaneous detection of aflatoxin B1 and type-B fumonisins in a single Test line, *Talanta*, 2019, **192**, 288–294, DOI: **10.1016/j.talanta.2018.09.037**.

29 A. Sena-Torralba, *et al.*, A Novel Ratiometric Fluorescent Approach for the Modulation of the Dynamic Range of Lateral Flow Immunoassays, *Adv. Mater. Technol*, 2101450, DOI: **10.1002/admt.202101450**.

30 Salimetrics, *Salivary Cortisol ELISA Kit*, 2021, **https://salimetrics.com/assay-kit/salivary-cortisol-elisa-kit/**.

31 LSBio, *Human Cortisol ELISA Kit*, **https://www.lsbio.com/elisakits/human-cortisol-competitive-eia-elisa-kit-ls-f10024/10024**.

32 E. H. Yee, S. Lathwal, P. P. Shah and H. D. Sikes, Detection of Biomarkers of Periodontal Disease in Human Saliva Using Stabilized, Vertical Flow Immunoassays, *ACS Sens.*, 2017, **2**, 1589–1593, DOI: **10.1021/acssensors.7b00745**.

33 P. Pearlmutter, *et al.*, Sweat and saliva cortisol response to stress and nutrition factors, *Sci. Rep.*, 2020, **10**, 19050, DOI: **10.1038/s41598-020-75871-3**.

34 R. Gatti, *et al.*, Cortisol assays and diagnostic laboratory procedures in human biological fluids, *Clin. Biochem.*, 2009, **42**, 1205–1217, DOI: **10.1016/j.clinbiochem.2009.04.011**.

35 K. Saha, F. Bender and E. Gizeli, Comparative Study of IgG Binding to Proteins G and A: Nonequilibrium Kinetic and Binding Constant Determination with the Acoustic Waveguide Device, *Anal. Chem.*, 2003, **75**, 835–842, DOI: **10.1021/ac0204911**.

36 J. Turkevich, P. C. Stevenson and J. Hillier, A study of the nucleation and growth processes in the synthesis of colloidal gold, *Discuss. Faraday Soc.*, 1951, **11**, 55–75, DOI: **10.1039/DF9511100055**.

37 G. Frens, Controlled Nucleation for the Regulation of the Particle Size in Monodisperse Gold Suspensions, *Nat. Phys. Sci.*, 1973, **241**, 20–22, DOI: **10.1038/physci241020a0**.

38 G. Tatulli and P. P. Pompa, An amplification-free colorimetric test for sensitive DNA detection based on the capturing of gold nanoparticle clusters, *Nanoscale*, 2020, **12**, 15604–15610, DOI: **10.1039/D0NR03517C**.

39 G. Maiorano, *et al.*, Monodispersed and size-controlled multibranched gold nanoparticles with nanoscale tuning of surface morphology, *Nanoscale*, 2011, **3**, 2227–2232, DOI: **10.1039/C1NR10107B**.